Desalination and Water Treatment
www.deswater.com
doi: 10.1080/19443994.2013.855669

53 (2015) 1578–1590
February

Defluoridation of groundwater using Fe^{3+}-modified bentonite clay: optimization of adsorption conditions

W.M. Gitari[a,*], T. Ngulube[a], V. Masindi[a], J.R. Gumbo[b]

[a] *Environmental Remediation and Water Pollution Chemistry Research Group, Department of Ecology and Resources Management, University of Venda, Private bag X5050, Thohoyandou, 0950 Limpopo, South Africa*
Tel. +27 15 962 8572; email: mugera.gitari@univen.ac.za
[b] *Department of Hydrology and Water Resources, School of Environmental Studies, University of Venda, Private bag X5050, Thohoyandou, 0950 Limpopo, South Africa*

Received 16 May 2013; Accepted 6 October 2013

ABSTRACT

Groundwater is the most appropriate and widely used source of drinking water for many rural communities in Sub-Saharan Africa. Studies reveal that in some of the boreholes, F^- concentration may be way beyond the recommended limits for drinking water. This study evaluates the use of raw unprocessed bentonite clay and its Fe^{3+}-modified form for fluoride adsorption. A series of batch adsorption experiments were carried out to evaluate parameters that influence the adsorption process. Loading of Fe^{3+} on bentonite was achieved by contacting the powdered clay with 80 ppm Fe^{3+} solution for 15 min at S/L ratio of 2 g/100 ml. The raw unprocessed bentonite clay was observed to increase the pH of the F^- solution as opposed to the Fe^{3+}-modified bentonite. Fe^{3+} bentonite exhibited ≈100% F^- removal as opposed to unprocessed bentonite <5% at initial concentration of 10 ppm F^-. The Fe^{3+}-modified bentonite exhibited ≈100% F^- removal over the pH range 2–10 decreasing at pH > 10, while the unprocessed raw bentonite clay showed release of F^- over the same pH range. This is crucial for the application of this adsorbent, since defluoridation can be carried out at the normal pH of the groundwater with no adjustment unlike most other adsorbents. The Fe^{3+}-modified bentonite was effective in F^- removal in high fluoride borehole water samples. The adsorption data fitted well to Langmuir adsorption model indicating a monolayer coverage of the adsorbent. The adsorption process was also observed to be favorable at room temperature. The results indicate that Fe^{3+}-modified bentonite has potential for application in groundwater defluoridation and more so as a candidate adsorbent for point of use water defluoridation systems for household use in rural areas in South Africa.

Keywords: Batch experiments; Groundwater; Defluoridation; Bentonite clay; Adsorption Isotherms; pH; Cation exchange capacity

1. Introduction

Safe drinking water is a necessity for every human being, clean portable water is scarce and not easily available. Non-palatability and non-portability of water may be due to natural geochemical factors or due to industrial activity. Due to a combination of factors, such as climate change, draught conditions, dwindling surface water resources, destruction of

---

*Corresponding author.

water catchment through deforestation. In most sub-Saharan countries, sources of clean surface water for most rural communities are diminishing by the day. Due to the decreasing surface water resources most rural communities are resulting to groundwater as the main source of their water.

Flouride ion is essential in human development specifically for the formation of teeth and bones if ingested at the correct concentration levels. However, too high fluoride intake normally gives rise to teeth mottling (dental fluorosis) and related problems [1]. The World Health Organization has set a guiding value of 1.5 mg/L for fluoride in drinking water [2], while the South African drinking water standard is also set at 1.5 mg/L [3].

Groundwater may be contaminated by fluoride through anthropogenic and natural sources. Fluoride can leach into groundwater resources from naturally occurring F^- containing mineral deposits such as fluorapatite [$3Ca_3(PO_4)_2Ca(F,Cl_2)$], sellaite (MgF_2), fluorspar (CaF_2), and cryolite (Na_3AlF_6) [4]. Research studies have documented strong correlation between dental fluorosis and high fluoride in ground and surface waters used by rural communities [5,6]. Studies carried out in South Africa have shown that the occurrence of dental fluorosis in the majority of cases are related to the fluoride content of groundwater used for drinking purposes [7]. Ncube and Schuttle [8] identified areas of high groundwater fluoride concentration in South Africa and related this to the occurrence of dental fluorosis in most communities using groundwater for domestic purposes. Dental fluorosis was observed in those areas with fluoride levels higher than the recommended guidelines for drinking water.

Many rural communities in South Africa and other sub-Saharan countries are increasingly using groundwater as the main source of drinking water. Mahumani [9] observes that groundwater is the main source of water for domestic and agricultural use in rural Limpopo province of South Africa. Meenakshi [1] points out that freshwater occurs as surface and groundwater and groundwater contributes only 0.6% of the total water resources on Earth, but it is the major source of drinking water in rural as well as urban areas particularly in developing countries. In addition, documented studies have revealed that in some of the boreholes, fluoride concentration may be way beyond the recommended limits for drinking water and will require defluoridation [8]. There is therefore a need to develop fluoride removal systems that are relatively simple, cost effective, and require low maintenance for use in the rural areas.

Major fluoride removal techniques developed so far include chemical precipitation [10], membrane processes [11], adsorption [12] and ion exchange [13]. Of all these technologies developed so far, adsorption has been considered as the most efficient and applicable technology for fluoride removal from ground and surface water in rural areas. Among the adsorbents tested, activated alumina is the most widely used because it is readily available and inexpensive. However, frequent regeneration with aluminium sulfate is required because of its low adsorption capacity at neutral pH [14,15], which results in increased difficulty for operation and poor sustainability in addition to increased dissolved aluminium in treated water. In addition, regeneration of the exhausted activated alumina requires trained technical personnel.

Research into the techniques available to defluoridate groundwater identifies those methods based on the principals of sorption as the methods most suited for rural and remote locations. The systems are relatively simple, requiring a reactor vessel to contain the media (which could be a simple column), which once it is exhausted can be regenerated or replaced. The challenge is to come up with a cheap and reliable adsorbent that can be effectively and cheaply regenerated. Several studies have identified locally available materials as the most suitable for evaluation and application for defluoridation in most rural communities, these include natural clay used for making of bricks [16], natural clay [17], raw bauxite [18], and natural lateritic geomaterials [19]. Most of these studies have insinuated that clay based materials obtained locally in rural areas affected by high fluoride in groundwater would be the most, the most economically viable adsorbents. Moreover, these materials could serve as good candidates for fabrication of point of entry or point of use water defluoridation systems that are suited for rural areas that are not connected to piped water supply.

Large specific surface area, chemical, and mechanical stability, layered structure, high cation exchange capacity (CEC), etc. have made some clays excellent adsorbent materials. Due to their great adsorptive properties, clays can be modified to create clay-based adsorbents for inorganic contaminants in water. This involves replacing the exchangeable cations such as Na^+, K^+. Ca^{2+}, and Mg^{2+} with high ionic charge density ions like Fe^{3+}, Mn^{2+}, or Al^{3+}. The modified clays have been observed to provide good abilities of adsorbing inorganic contaminants [20]. Onyango et al. [21] observed a greater F^- adsorption capacity for Al^{3+} zeolite F9 modified zeolite compared to commercial adsorbents. Kamble et al. [22] observed a higher F^- adsorption capacity for La^{3+}, Mg^{2+}, and Mn^{2+}-modified bentonite compared to the unmodified one. The objectives of this paper includes: (1) physicochemical and mineralogical characterization of the raw and modified bentonite clay, (2) optimizing the loading of Fe^{3+} onto bentonite clay, (3) optimization of the F^- adsorption capacity of the raw and modified bentonite clay, and (4) evaluate the F^-adsorption capacity of the raw and modified bentonite clay at optimized conditions for natural high fluoride groundwater.

2. Materials and methods

2.1. Preparation of bentonite clay samples

The raw bentonite samples were washed with ultra-pure water (Millipore, USA). The washed bentonite was then dried in an oven for 24 h at a temperature of 105 ℃. The dried sample was crushed into a fine powder (passing through a 32 μm sieve).

2.2. Physicochemical and mineralogical characterization of bentonite samples

2.2.1. X-ray fluorescence (XRF) and X-ray diffraction analysis

Major and minor elemental analysis of the prepared powdered bentonite samples was done by a PAN analytical Axios X-ray fluorescence spectrometer equipped with a 4 kW Rh tube at Council for Geoscience, South Africa. Powdered previously washed and dried bentonite samples were used for X-ray diffraction analysis (XRD). A weighed amount of the powdered bentonite samples were prepared for XRD analysis, using a back loading preparation method.They were analyzed using a PANalytical X'Pert Pro powder diffractometer with X'Celerator detector and variable divergence and receiving slits with Fe filtered Co-Kα radiation. The phases were identified using X'Pert Highscore plus software. The relative phase amounts (weight %) were estimated using the Rietveld method (Autoquan Program). A Vernier was used to measure the d-spacing of the peaks which were then compared with those in the Hanawalt index.

2.2.2. Cation exchange capacity

The CEC of the raw unprocessed and Fe^{3+}-modified bentonite clay samples was done by extracting the exchangeable cations using 1 M ammonium acetate buffer at pH 7.4 and pH 5.4. The concentration of the exchangeable cations (Ca^{2+}, Mg^{2+}, K^+, and Na^+) was determined by Atomic Absorption Spectrometer (600 Perkin–Elmer). The results in ppm were then converted to meq per 100 g of sample following the method of Radojevic and Bashkin [23].

2.2.3. Scanning electron microscopy analysis

The morphology of the raw bentonite and Fe^{3+}-reacted bentonite was examined using a Hitachi X-650 scanning Electron Microanalyser equipped with a CDU-lead detector at 25 kV. Samples were mounted on aluminum pegs and coated with a thin film of gold to make them conductive.

2.2.4. The determination of pH_{pzc}

Batch equilibrium experiments were used to estimate the point of $pH_{pzc.}$ Forty-five millilitres of 0.1 M KCl solution were transferred to 8, 50 mL calibrated bottles and capped. The initial pH ($pH_{initial}$) of the solutions was adjusted in the range of 2–12.0 by adding 0.1 M HCl and 0.1 M NaOH solutions. The total volume of the solution in each bottle was adjusted exactly to 50 mL by adding the KCl solution of the same strength. 1 g of dry bentonite clay was added to each bottle and the suspensions then equilibrated for 24 h. After equilibration time, the solutions were filtered and final pH values (pH_{final}) of the filtrates measured. The difference between initial and final pH (pH_f) values ($\Delta pH = pH_i - pH_f$) was plotted against pH_i. The point of intersection of the resulting curve with abscissa (the co-ordinate that gives the distance along the horizontal axis), at which $\Delta pH = 0$, was an indication of the point of zero charge. Same procedure was repeated twice but replacing the electrolyte with 0.01 M and 0.001 M KCl solution.

2.2.5. BET analysis

The surface area and pore size distribution of raw and modified bentonite clay were determined using the Brunnet–Emmett–Teller method of analysis using a Micromeritics Accelerated Surface Area and Porosimetry (ASAP) 2010 system [24]. Nitrogen adsorption isotherms were obtained at liquid nitrogen temperature. Prior to the determination of the adsorption isotherm, the samples were degassed and approximately 10 g of raw and modified bentonite clay were subjected to degassing at 120 ℃ for 24 h. The degassing process was meant to remove adsorbed gases and moisture. The raw and Fe^{3+}-modified bentonite clay was then placed in a N_2 stream and the mass change of the solid due to gas adsorbed was measured relatively to the change in partial pressure of N_2.

2.3. Modification and synthesis of Fe^{3+}-modified bentonite clay

The Fe^{3+}-modified bentonite for the defluoridation experiments was synthesized using the conditions optimized in previous experiments [25]. A 500 mL, 100 ppm Fe^{3+} solution was mixed with 15 g of bentonite to make up a L/S ratio of 100 mL/3 g. The mixture was put on a 1,000 mL Erlenmeyer flask in order to avoid spillage during agitation. The mixture was agitated for 15 min at 250 rpm on a table shaker and filtered. The solid residue left on the filter paper was dried for 12 h at a temperature of 105 ˚C in the oven. The material was then ground to a fine powder and used for subsequent defluoridation experiments. The experiments were repeated three times to generate enough Fe^{3+}-modified bentonite for subsequent experiments.

2.4. Optimization of F^- adsorption conditions

2.4.1. Adsorption as a function of contact time

Adsorption of F^- with contact time was evaluated by use of 10 ppm F^- solution and 2 g/100 mL S/L ratio. Samples were agitated at 250 rpm using a table shaker. Samples were shaken for various time intervals ranging from 1 to 360 min. Samples were filtered through 0.45 μm pore cellulose nitrate membranes. pH, EC, and TDS were measured using crimson multimeter probe and F^- by crimson ion selective electrode. Reactions were carried out at room temperature.

2.4.2. Adsorption as function of adsorbent dosage

Adsorption of F^- with adsorbent dosage was evaluated by use of 10 ppm F^- solution. The adsorbent dosage was varied as follows: 0.1, 0.3, 0.5, 1, 2, 3, and 4 g. Samples were agitated for 30 min at 250 rpm using a table shaker and filtered through 0.45 μm pore cellulose nitrate membranes. pH, EC, and TDS were measured using crimson multimeter probe and F^- by crimson ion selective electrode. Reactions were conducted at room temperature.

2.4.3. Adsorption as a function of adsorbate concentration

Adsorption of F^- with adsorbate concentration was evaluated at 30 min contact time and agitated at 250 rpm using a table shaker. A S/L ratio of 2 g/100 mL was used, adsorbate concentration was varied from 4 to 60 ppm. Samples were filtered through 0.45 μm pore cellulose nitrate membranes. pH, EC, and TDS were measured using crimson multimeter probe and F^- by crimson ion selective electrode. Reactions were conducted at room temperature.

2.4.4. Adsorption as a function of pH

Adsorption of F^- as a function of pH was evaluated at 20 ppm F^- concentration. Agitation was done for 30 min contact time at 250 rpm using a table shaker. A S/L ratio of 2 g/100 mL was employed. Initial pH of the media was varied from 2 to 12. Samples were filtered through 0.45 μm pore cellulose nitrate membranes. pH, EC, and TDS were measured using crimson multimeter probe and F^- by crimson ion selective electrode. Reactions were conducted at room temperature.

2.4.5. Adsorption of F^- in borehole water at the optimized conditions

The optimized conditions of 30 min of contact time, 2 g/100 ml of adsorbent dosage, 250 rpm, and a pH of 2 established in the optimization stage were applied for the defluoridation of Siloam borehole water.

2.4.6. Calculation of % adsorption and adsorption capacity

The percentage of fluoride removal by raw and Fe^{3+}-modified bentonite clay was computed by use of the following Eq. (1).

$$\%\ \text{Removal} = \left(\frac{C_0 - C_e}{C_0}\right) \times 100 \tag{1}$$

where: C_0 initial concentration and C_e equilibrium F^- concentration, respectively.

The adsorption capacity of raw and Fe^{3+}-modified bentonite clay for fluoride (q) was computed using Eq. (2).

$$q = \frac{(C_i - C_e)V}{m} \tag{2}$$

where: C_i = initial fluoride concentration (mg/L); C_e = F concentration at equilibrium (mg/L); V = Volume of F− solution (L); m = weight of adsorbent (g).

3. Results and discussions

3.1. Chemical and mineralogical characterization of raw and Fe^{3+}-modified bentonite clay

Table 1 presents the major chemical constituents of raw washed bentonite and CEC, respectively. The high concentration of SiO_2 and Al_2O_3 confirms that bentonite is an alumino-silicate material. The relatively high concentrations of MgO, Na_2O, CaO, and K_2O indicates that Mg^{2+}, Na^+, Ca^{2+}, and K^+ are the main exchangeable cations. This is confirmed by the subsequent decrease of the content of these chemical species in the Fe^{3+}-modified bentonite clay.

The raw bentonite and the Fe^{3+}-modified bentonite consists of significant minor chemical species such as F^-, Sr, Ba, Zr, and Cl^- that could be released in the reaction mixture during the adsorption process. An increase in Fe content is observed for the Fe^{3+}-modified bentonite clay confirming the loading of Fe^{3+} in the interlayers. Fig. 1 shows the XRD spectrum of raw bentonite clay and indicates the minerals present. Quantitative XRD further confirmed that it contains montmorillonite (74.76%) as the major mineral phases with minor quantities of quartz (15.98%), plagioclase (8.17%), and muscovite (1.09%).

3.2. Cation exchange capacity and point of zero charge

Table 2 shows the concentration of the exchangeable cations and the calculated CEC of the raw bentonite and Fe^{3+}-modified bentonite clay at pH 7.4 and 5.4 of the extracting media.

Reaction of the bentonite with Fe^{3+} solution leads to a reduction of CEC indicating the main mechanism of Fe^{3+} uptake is by ion exchange. The CEC results also confirm that the main exchangeable cation is Na^+. Change of pH of the buffering media does not seem to have any effect on the exchangeable cations concentration and subsequently the CEC. Fig. 2 shows the pH_{pzc} of raw and modified bentonite clay. It is observed that there is an increase in pH_{pzc} on introduction of Fe^{3+} cations (Raw bentonite: 8.2 and Fe^{3+}-modified bentonite clay: 8.5).

Both raw and Fe^{3+}-modified bentonite clay have high pHpzc characteristic of clay materials dominated by aluminosilicate materials and iron oxides. Modification of the raw bentonite clay with Fe^{3+} increases the pHpzc and which extends the pH range for adsorption of anions meaning that the Fe^{3+}-modified bentonite clay will have high adsorption capacity for anions than the raw bentonite clay.

Table 1
Chemical composition of the raw and Fe^{3+}-modified bentonite

Major oxides (% by weight)			Minor and traces (mg/kg)		
Chemical species	Raw bentonite	Fe^{3+}-bentonite	Chemical species	Raw bentonite	Fe^{3+}-bentonite
SiO_2	66.51	67.26	As	6.25	12.21
TiO_2	0.14	0.13	Cu	2.00	2.00
Al_2O_3	16.81	16.99	Ga	11.01	9.20
Fe_2O_3	3.26	3.76	Mo	1.00	1.00
MnO	0.13	0.13	Nb	2.00	2.00
MgO	3.12	3.12	Ni	3.00	3.00
CaO	1.43	1.33	Pb	15.15	13.09
Na_2O	1.17	0.43	Rb	2.00	2.00
K_2O	0.54	0.46	Sr	14.58	5.52
P_2O_5	0.03	0.03	Th	3.00	3.00
Cr_2O_3	<0.01	<0.01	U	3.00	3.00
LOI	7.19	6.96	W	6.00	6.00
Total	100.35	100.62	Y	3.00	3.00
			Zn	30.15	27.65
			Zr	75.36	55.19
			Cl	7.58	7.58
			Co	2.36	2.36
			F	100.00	100.00
			S	16.00	16.00
			V	16.81	16.81
			Cs	36.64	28.68
			Ba	353.18	407.26
			La	41.94	50.34
			Ce	82.34	86.50

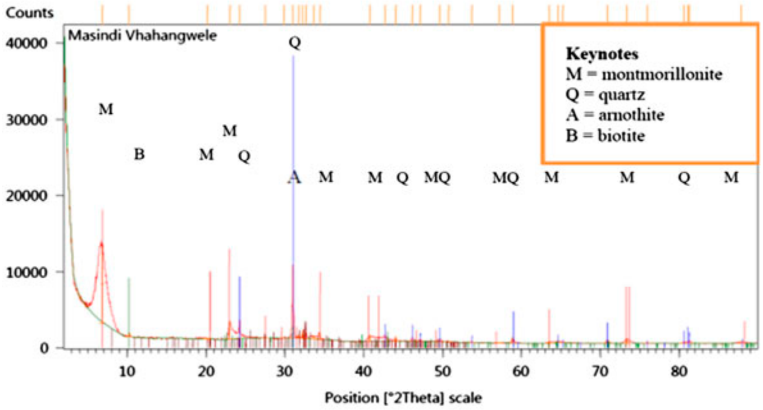

Fig. 1. XRD diffractogram of raw bentonite clay.

Table 2
CEC of raw and Fe^{3+}-modified bentonite clay at pH 5.4 and 7.4

	Exchangeable chemical species (mg/l)				
	Na^+	K^+	Ca^{2+}	Mg^{2+}	CEC (meq/100 g)
Raw bentonite/pH					
5.4	115.2	3.3	57.1	86.4	262
7.4	117.7	3.7	56.2	97.9	265.5
Fe^{3+}-bentonite/pH					
5.4	49.2	2.8	57.8	85.7	195.5
7.4	46.6	2.6	56.8	82.9	188.9

3.3. Morphology and surface area determination

Fig. 3 shows the SEM images of washed raw bentonite and the bentonite after interacting with the Fe^{3+} solution. No difference in morphology of the raw bentonite and the Fe^{3+}-modified bentonite was observed (Fig. 3). The platy-like features characteristics of clay minerals are clearly visible.

An important physical property of clay minerals is their high surface areas. Total surface area depends on both internal and external surface areas. Table 3 shows the BET-N_2 determined surface areas and micropore volumes of the raw and Fe^{3+}-modified bentonite clay.

The BET-N_2 surface area represents the total surface area (external surface area + micropore area). An increase in the surface area and micropore volume is observed for Fe^{3+}-modified bentonite clay as compared to the bentonite. This could be an indication of propping up of the interlayers by the solvated $[Fe(H_2O)_6]^{3+}$. An increase in the external surface area could be due to surface adsorption and surface precipitation of Fe^{3+} from solution. An increase in surface area makes the Fe^{3+}-modified bentonite clay a better adsorbent than the raw bentonite clay.

3.4. Defluoridation of water using the raw and Fe^{3+}-modified bentonite clay: optimization of F^- adsorption conditions

3.4.1. Fluoride removal as a function of contact time

Fig. 4(a–d) presents the variation of pH, F^-, EC, TDS with time for raw and Fe^{3+}-modified bentonite clay. The TDS and EC increased with contact time for the raw bentonite (Fig. 4(b)) indicating possible release of soluble chemical species in solution. The raw

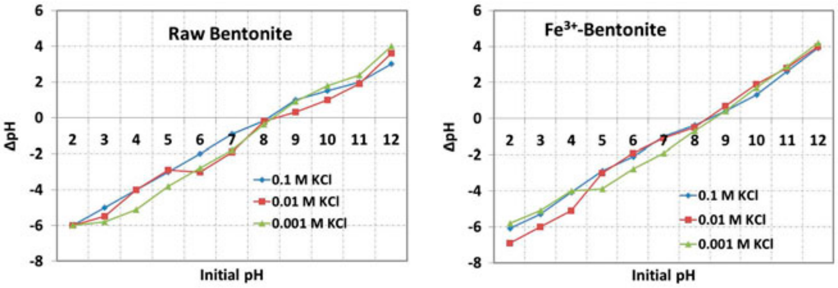

Fig. 2. pH_{pzc} of raw bentonite and Fe^{3+}-modified bentonite clay.

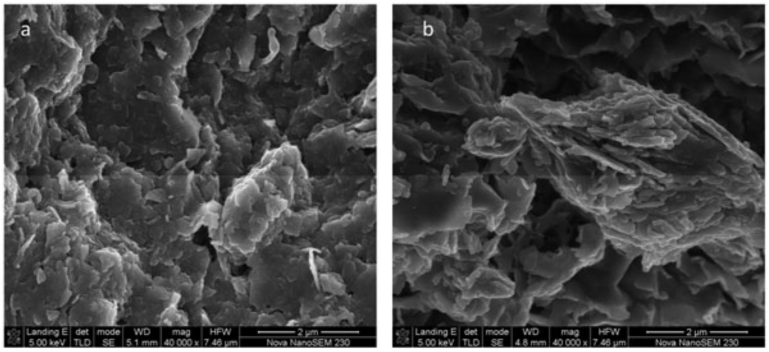

Fig. 3. SEM micrographs of washed raw bentonite (a) and Fe^{3+}-modified bentonite (b).

Table 3
BET surface, external surface area, and micropore areas and micropore volume of raw bentonite and Fe^{3+}-modified bentonite clay

Sample	BET surface area (m^2/g)	External surface area (m^2/g)	Micropore area (m^2/g)	Micropore vol (cm^3/g)
Raw bentonite	16.015	11.088	4.926	0.002
Fe^{3+}-bentonite	49.953	37.416	12.536	0.0054

bentonite seems to increase the pH of the solution through possible dissolution of alkaline metal oxides (Table 1 and Fig. 4(a)). In addition raw bentonite seems to release F^- into solution, XRF results showed presence of F in the raw bentonite (Table 1).

Despite initial high EC and TDS levels for the Fe^{3+} bentonite reaction mixture the EC and TDS stabilizes at the same level as raw bentonite for the entire contact time. Fe^{3+}-bentonite reduces the F^- to below 1 ppm within one minute. This clearly indicates changes in the physicochemical and surface properties of the bentonite clay on introduction of Fe^{3+} ions. Thereafter, F^- concentration stabilized at values less than 1 ppm, while pH stabilized at 3.5 at 30 min of contact time. Thirty minutes of contact time taken as the optimum contact time and was applied in subsequent experiments.

3.4.2. Fluoride removal as a function of adsorbent dosage

Fig. 5(a–d) shows the variation of pH, F^-, EC, and TDS with adsorbent dosage for raw and Fe^{3+}-modified bentonite clay. An observation of Fig. 5(a) shows that raw bentonite actually releases F^- into solution; this is observed to increase with adsorbent dosage. pH also increases with adsorbent dosage confirming release of OH^- in solution through possible dissolution of alkaline metal oxides (Table 1). On the contrary the Fe^{3+}-modified bentonite clay decreases the F^- content to below 1 ppm at 1 g adsorbent dosage. The pH decreases with increase of adsorbent dosage. The Fe^{3+}-modified bentonite clay could be releasing H^+ to compensate for the adsorbed F^- ions, hence lowering pH or the hydrolysis of the hydrated $[Fe(H_2O)_6]^{3+}$ in the bentonite interlayers (Eq. (3)).

$$[Fe(H_2O)_6]^{3+} \Rightarrow [Fe(H_2O)_5OH]^{2+} + H^+ \tag{3}$$

3.4.3. Fluoride removal as a function of adsorbate concentration

Fig. 6(a–d) shows the % F^- adsorption, final F^- concentration as a function of adsorbate concentration.

Fig. 6(a) shows the % F^- adsorption as a function of the adsorbate concentration for the raw bentonite. Raw bentonite is observed to release F^- in the reaction mixture and this is observed to be high at lower adsorbate concentration (4–10 ppm) (Fig. 6(a) and (c)). Fe^{3+}-modified bentonite shows efficient adsorption, removing >98% of F^- even as the adsorbate concentrations increases to 60 ppm (Fig. 6(b) and (d)).

3.4.4. Fluoride removal as a function of initial pH

Fig. 7(a) and (b) shows the final concentration of F^- in the residual water as a function of the initial pH.

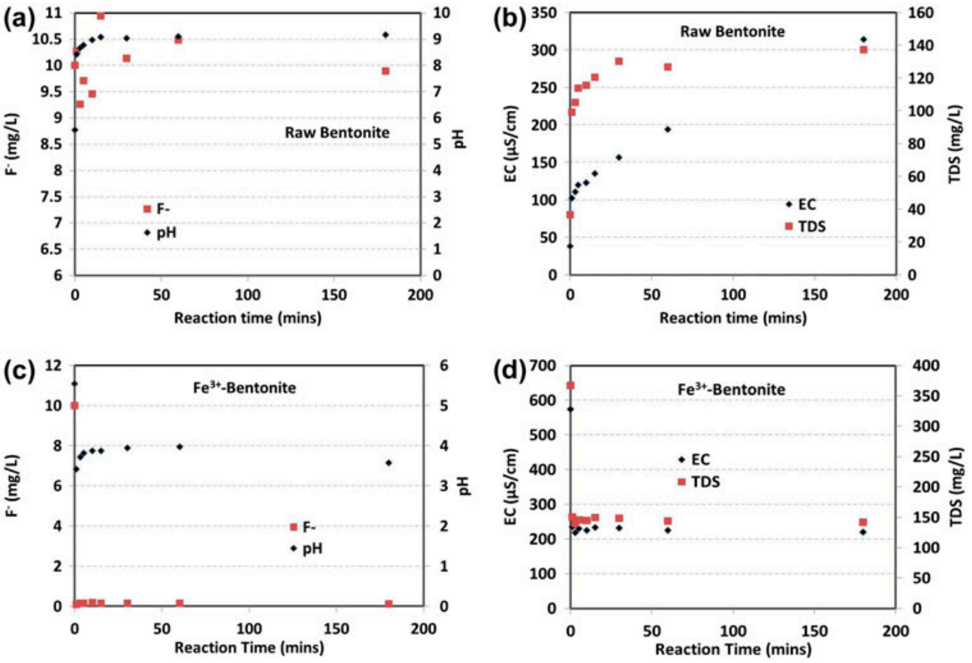

Fig. 4. Variation of F^-, pH, EC, and TDS with contact time for raw and Fe^{3+}-modified bentonite clay (2 g/100 ml, 10 ppm F^-, pH = 5.54, agitation speed = 250 rpm and 26 ℃).

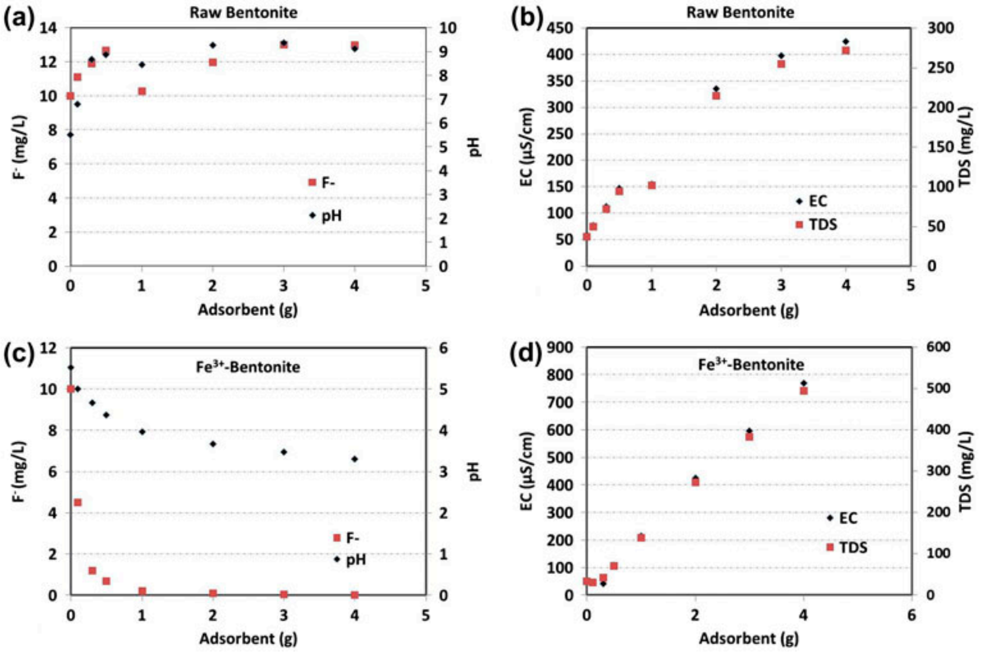

Fig. 5. Variation of pH, F^-, EC, and TDS with adsorbent dosage for raw and Fe^{3+}-modified bentonite clay (contact time = 30 min, vol = 100 ml, 10 ppm F^-, pH = 5.53, agitation speed = 250 rpm and 26 ℃).

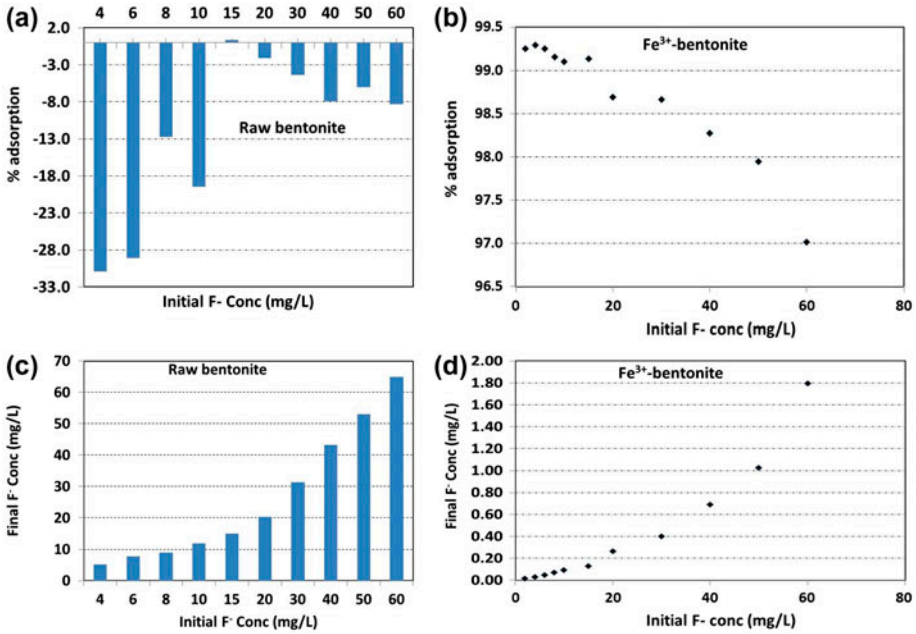

Fig. 6. Variation of % F^- adsorption, equilibrium F^- concentration as a function of adsorbate concentration (contact time = 30mins, 2 g/100 ml, pH = 5.3, agitation speed = 250 rpm, conc 4–60 ppm, and 26 ℃).

Both raw and Fe^{3+}-modified bentonite clay shows high removal of F^- at low pH 2 (Fig. 7(a, b)). Raw bentonite however shows no adsorption of F^- at pH 4–10 and at pH 12, it releases F^- into residual solution. Fe^{3+}-modified clay show strong adsorption of F^- at pH range of 2–10, but at pH 12 the F^- remains largely in solution. A slight decrease is observed at pH 6–10, this is attributed to the change in surface charge as the pH of the solution approaches pHpzc (8.5) for Fe^{3+}-modified bentonite clay. The low adsorption at highly alkaline pH could be due to the competition of adsorption sites with OH^- and due to the fact that the surface of the clay is negatively charged and there is increased electrostatic repulsion of the anionic fluoride as the pH > pHpzc (8.5) for the Fe^{3+}-modified bentonite clay. The mechanism of adsorption of F^- by the Fe^{3+}-modified bentonite clay seems to involve largely the interaction of the F^- ion with the hydrated Fe^{3+} ion in the bentonite interlayers (Eq. (4)).

$$\begin{aligned}
&[Fe(H_2O)_6]^{3+} \Rightarrow [Fe(H_2O)_3(OH)_3] + 3H^+]\\
&[Fe(H_2O)_3(OH)_3] + F^- \Rightarrow [Fe(H_2O)_3(OH)_2(F)] + OH^-\\
&[Fe(H_2O)_3(OH)_2(F)] + F^- \Rightarrow [Fe(H_2O)(OH)(F)_2] + OH^-
\end{aligned} \tag{4}$$

The fact that the pH range of maximum adsorption cuts across the pHpzc (8.5) seems to indicate the surface/edge adsorption of F^- contribution to total F^- removal is minimal. At pH 2 the surface of the clay is

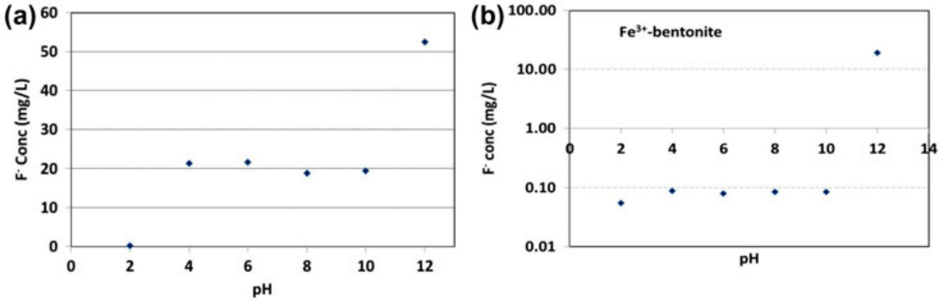

Fig. 7. Variation of equilibrium F^- concentration as a function of pH (contact time = 30 min, 2 g/100 ml, 10 ppm F^-, agitation speed = 250 rpm and 26 ℃).

positively charged and F^- would be electrostatically attracted to the clay surface which explains the high F^- adsorption. However, as pH increases to 4 there is increased OH^- ions that compete with F^- for adsorption sites. This explains the slight decrease in F^- adsorption over the pH range 4–10 (Fig. 7(b)) and no adsorption at pH 12.

3.6. Adsorption of F^- for groundwater using Fe^{3+}-modified bentonite clay at natural pH and at optimized pH conditions

Table 4 shows the adsorption of fluoride from Siloam borehole water by Fe^{3+}-modified bentonite clay at optimized pH and natural conditions. The physicochemical characteristics of the groundwater water samples before and after defluoridation are also shown in Table 4. The groundwater water was slightly alkaline having a pH of 8.75.

The potential of Fe^{3+}-modified bentonite clay for defluoridation of groundwater was tested in natural groundwater samples collected from the borehole in the fluoride-affected area (Siloam Village) in Limpopo province, South Africa. The fluoride removal efficiency in the ground water at natural pH conditions and at optimized pH conditions was not significantly different (Table 4). This could be due to the fact that the natural pH of the groundwater (8.75) was within the optimized pH range (2–10) for defluoridation of the groundwater using Fe^{3+}-modified bentonite clay. At both natural and optimized pH conditions, the Fe^{3+}-modified bentonite clay was able to remove the excess fluoride concentrations to below the WHO water quality guidelines. However, the pH was observed to drop to below the required standard of 6–9. This would be a shortcoming, since the treated water would require pH adjustment. Therefore, it can be concluded that Fe^{3+}-modified bentonite clay is an effective adsorbent for fluoride.

Table 4
Defluoridation of groundwater using Fe^{3+}-modified bentonite clay at natural pH and at optimized pH conditions

Parameter	Siloam borehole water	Natural conditions	Optimized conditions	WHO guidelines
pH	8.75	1.95	2.92	6–9
EC (μS/cm)	99	321	159.9	0–150
TDS (mg/l)	63.4	205	102.3	0–500
F^- (mg/l)	8.499	0.067	0.032	1.5

4. Adsorption isotherms

The raw bentonite clay was observed to be a poor adsorbent for F^- and actually was observed to release F^-. Further, discussion of the results was restricted to the Fe^{3+}-modified bentonite clay. The adsorption capacity Q_e (mg/g) of the Fe^{3+}-modified bentonite clay was evaluated by determining equilibrium sorption of F^- as a function of concentration at the pH of the F^- solution. The variation of adsorption capacity of Fe^{3+}-modified bentonite clay for F^- is presented in Fig. 8.

It is observed that the adsorption capacity at equilibrium gradually increases at low adsorbate concentration which indicates availability of excess adsorption sites. However, as the adsorbate concentration increases the adsorption capacity at equilibrium gradually decreases until it flattens off indicating saturation. At this high adsorbate concentration, the availability of adsorption sites becomes the limiting factor as the adsorbent surface reaches maximum adsorption capacity. Maximum adsorption capacity was observed to be 2.91 mg/g.

The equilibrium data was further processed using two commonly used isotherms: Langmuir and Freundlich. The Langmuir isotherm theory assumes monolayer coverage of adsorbate over a homogenous adsorbent surface, i.e. the surface consists of identical sites equally available for adsorption and with equal energies of adsorption [25]. It is represented as (Eq. (5)):

$$q_e = \frac{q_m K_a C_e}{1 + K_a C_e} \tag{5}$$

where C_e is the equilibrium concentration (mg/L), q_e is the amount of adsorbate adsorbed (mg/g), q_m is q_e for a complete monolayer (mg/g), K_a is the adsorption

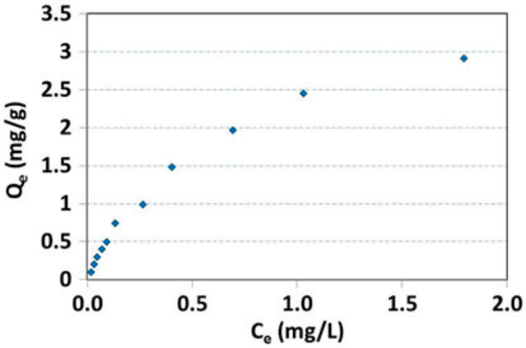

Fig. 8. Adsorption isotherm of fluoride sorption on Fe^{3+}-modified bentonite clay (contact time = 30 min, adsorbent dose = 2 g/100 ml, pH = 5.3; agitation speed = 250 rpm, 26 ℃, conc 4–60 ppm).

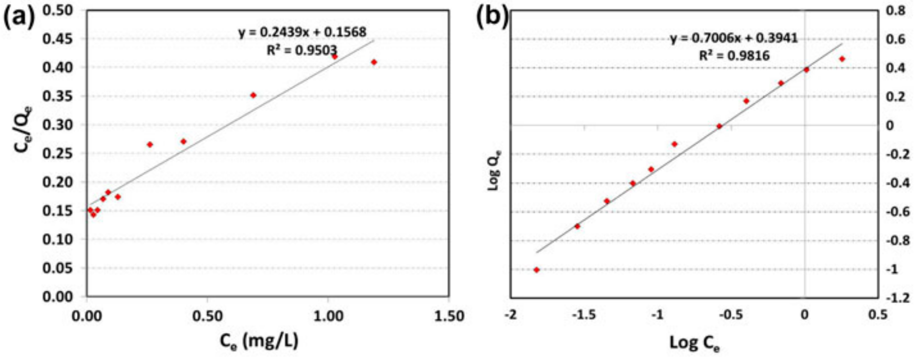

Fig. 9. Langmuir (a) and Freundlich (b) adsorption isotherms obtained by the linear method for the fluoride adsorption onto Fe^{3+}-modified clay (contact time = 30 min, adsorbent dose = 2 g/100 ml, pH = 5.3; agitation speed = 250 rpm, 26 ℃, conc 4–60 ppm).

equilibrium constant (L/mg), and is related to energy of adsorption. The constants q_m and K_a can be determined from a linear form of Eq. (3) as shown (Eq. (6)).

$$\frac{C_e}{q_e} = \frac{1}{q_m} C_e + \frac{1}{K_a q_m} \tag{6}$$

Freundlich isotherm is based on multilayer adsorption on heterogeneous surface and is represented as (Eq. (7)):

$$q_e = K_f C_e^{1/n} \tag{7}$$

where K_f and *1/n* are constants indicating the adsorption capacity and adsorption intensity, respectively. The linear form of the equation can be obtained by taking logarithms of Eq. (5) as shown (Eq. (8)):

$$\log q_e = \log K_f + 1/n \log C_e \tag{8}$$

The Langmuir and Freundlich adsorption isotherms for the F^- adsorption on Fe^{3+}-modified bentonite clay are presented in Fig. 9.

It can be observed that Langmuir isotherm (Fig. 9(a)) (r^2 = 0.9857) better describes the data than the Freundlich isotherm (Fig. 9(b)) (r^2 = 0.9816). This indicates that the F^- adsorption system was more likely a monolayer coverage of the Fe^{3+}-modified bentonite clay. The essential features of the Langmuir isotherm can also be expressed in terms of a dimensionless constant, separation factor or equilibrium parameter K_R which is defined by the following relationship (Eq. (9)):

$$K_R = \frac{1}{1 + K_a C_0} \tag{9}$$

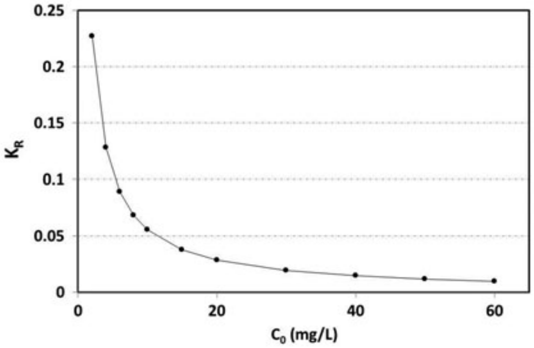

Fig. 10. Values of the separation factor, K_R for the adsorption of fluoride onto Fe^{3+}-modified bentonite clay.

where K_R is a dimensionless separation factor, C_0 is the initial fluoride concentration (mg/L), and K_a the Langmuir constant (L/mg). The parameter K_R indicates isotherm shape as follows $K_R > 1$: unfavorable, $K_R = 1$: linear, $0 < K_R < 1$: favorable, $K_R = 0$: irreversible. K_R values were calculated over the initial fluoride concentration range (4–60 ppm) used to generate the Langmuir adsorption isotherm (Fig. 10).

The calculated K_R values (Fig. 10) lie within the range 0–1 indicating adsorption process was favorable at room temperature (26 ℃) for all the adsorbate concentrations tested.

5. Conclusions and recommendations

Raw bentonite was successfully modified by adsorption of Fe^{3+} from aqueous solution. Optimum loading was observed at 30 min of agitation using 100 ppm Fe^{3+}solution.

Modification of the bentonite with Fe^{3+} increased the surface area and micropore area of the bentonite clay. Fe^{3+} bentonite was observed to be a suitable adsorbent for F^- from aqueous solution as compared to raw bentonite. The removal of F^- from aqueous solution was observed to strongly depend on the contact time, pH of the solution, and amount of adsorbent. Raw bentonite was observed to be ineffective in the adsorption of F^- from the aqueous solution, it was observed to release F^- in the solution and this was more pronounced at alkaline pH > 10. The results reveal that Fe^{3+}-modified bentonite clay is a potentially strong adsorbent for F^- removal in groundwater; moreover, the F^- removal was ≈100% over a wide pH range of 2–10. However, pretreatment of the raw bentonite before modification should be investigated with a view to removing the residual fluoride in the clay matrix. The adsorption capacity of Fe^{3+}-modified bentonite clay was established to be 2.91 mg/g. The adsorption data fitted well to Langmuir adsorption model indicating a monolayer coverage of the adsorbent. The adsorption process was also observed to be favorable at room temperature. Application of the Fe^{3+}-modified bentonite clay for defluoridation of groundwater at natural pH conditions and optimized pH conditions proved efficient in removing fluoride to below WHO limits. However, the pH dropped to below the required limits and the treated water will require pH adjustment.

Acknowledgments

The authors wish to express their gratitude to University of Venda Research and Innovation Directorate, Department of Ecology and Resources Management, ESKOM-TESP for the support and funding of this study.

References

[1] R.C.M. Meenakshi, Fluoride in drinking water and its removal, J. Hazard. Mater. B137 (2006) 456–463.

[2] WHO, Guidelines for Drinking Water Quality, World Health Organization, Geneva, 2004.

[3] Department of Water Affairs and Forestry (DWAF), South African Water Quality Guidelines for Domestic Use, 1st ed., Department of Water Affairs and Forestry, Pretoria, 1996. Available from: www.dwaf.gov.za.

[4] M. Mohapatra, S. Anand, B.K. Mishra, E.G. Dion, P. Singh, Review of fluoride removal from drinking water, J. Environ. Manage. 91 (2009) 67–77.

[5] R.K. Daw, Experiences with domestic defluoridation in India. People Centred Approaches to Water and Sanitation. 30th WEDC International Conference, Vientiane, Lao PDR (2004).

[6] M.W.K. Nyaora, M.P. Tole, T.C. Davies, The contribution of drinking water towards dental fluorosis: A case study of Njoro Division, Nakuru District. Kenya, Environ. Geochem. Health. 24 (2001) (2001) 123–130.

[7] WRC, Distribution of Fluoride-Rich Groundwater in the Eastern and Mogwase Regions of the Northern and North-West Province.WRC Report No. 526/1/01 1.1 9.85 (2001) Pretoria. South Africa. Available from: www.wrc.org.za.

[8] E.J. Ncube, C.F. Schuttle, The occurrence of fluoride in South African groundwater. A water quality and health problem, Water SA. 31 (2005) 35–40.

[9] B.K. Mahumani, The rural and agricultural value of groundwater as an economic resource in the Limpopo Region. MSc Thesis. University of Stellenbosch, Stellenbosch, South Africa, 2009.

[10] S. Saha, Treatment of aqueous effluent for fluoride removal, Water Res. 27 (1993) 1347–1350.

[11] A.G. Pervov, E.V. Dudkin, O.A. Sidorenko, V.V. Antipov, S.A. Khakhanov, R.I. Makarov, Membrane systems for drinking water production and their maintenance techniques, Desalination 132 (2000) 315–321.

[12] S. Ghorai, K.K. Pant, Investigations on the column performance of fluoride adsorption by activated alumina in a fixed-bed, Chem. Eng. J. 98 (2004) 165–173.

[13] S.Z. Qureshi, M.A. Khan, N. Rahman, Removal of fluoride ion by zirconium (IV) arsenate vanadate using ion selective electrode, Water Treat. 10 (1995) 307–312.

[14] S.A. Wasay, M.J. Haron, S. Tokunaga, Adsorption of fluoride, phosphate, and arsenate ions on lanthanum-impregnated silica gel, Water Environ. Res. 68 (1996) 295–300.

[15] H. Lounici, L. Addour, D. Belhocine, H. Grib, S. Naicolas, B. Bariou, N. Mameri, Study of a new technique for fluoride removal from water, Desalination 114 (1997) 241–251.

[16] A. Argaw, F. Kebede, Development of appropriate defluoridation technologies for Ethiopian communities, J Civil. Eng. J KUAT 8 (2005) 79–88.

[17] H. Ahmedin, Selection of clay adsorbents and determination of the optimum condition for defluoridation of groundwater in rift valley region. MSc Thesis. Department of Chemical Engineering, Addis Ababa University, Ethiopia, 2007.

[18] S. Sajidu, K. Chikumbusho, M. Wellington, M. Jonas, Defluoridation of groundwater using raw bauxite: rural domestic defluoridation technology, Environ. Nat. Res. 2 (2012) 1–9.

[19] M. Sarkar, B. Aparna, P.P. Partha, R.S. Asit, Design and operation of fixed bed laterite column for the removal of fluoride from water, Chem. Eng. J. 131 (2007) 329–335.

[20] B. Lothenbach, G. Furrer, R. Schulin, Immobilization of heavy metals by polynuclear aluminium and montmorillonite compounds, Environ. Sci. Technol. 31 (1997) (1997) 1452–1462.

[21] S.M. Onyango, Y.L. Taile, O. Aoyi, K. Dalibor, O.O. Fred, M. Hitoki, Breakthrough analysis for water defluoridation using surface-tailored zeolite in a fixed bed column, Ind. Eng. Chem. Res. 48 (2009) 931–937.

[22] S.P. Kamble, P. Dixit, S.S. Rayalu, N.K. Labhsetwar, Defluoridation of drinking water using chemically modified bentonite clay, Desalination 249 (2009) 687–693.

[23] M. Radojevic, V.N. Bashkin, Practical Environmental Analysis. The Royal Society of Chemistry, Cambridge, 1999, p. 466.

[24] S. Brunauer, The adsorption of gases and vapours. Princeton, Princeton University press, 1943.

[25] V.Masindi, Adsorption of oxyanions of As, B, Cr, Mo and Se from coal fly ash leachates using Al^{3+}/Fe^{3+} modified bentonite clay. Unpublished MSc Thesis. University of Venda, Thohoyandou, South Africa, 2013.

[26] M.A. Ahmad, N.K. Rahman, Equilibrium, kinetics and thermodynamics of Remazol Brilliant Orange 3R dye adsorption on coffee husk-based activated carbon, Chem. Eng. J. 170 (2011) 154–161.